Journal of Vegetation Science ■■ (2014)

Using imaging spectroscopy to predict above-ground plant biomass in alpine grasslands grazed by large ungulates

Anna K. Schweiger, Anita C. Risch, Alexander Damm, Mathias Kneubühler, Rudolf Haller, Michael E. Schaepman & Martin Schütz

Keywords
Consumption; Ecological scale; Heterogeneous; Quantity; Remote sensing; Swiss Alps

Abbreviations
ANPP = aboveground net primary productivity; ANPP_t = tall-grass aboveground net primary productivity; APEX = Airborne Prism Experiment (imaging spectrometer); FUO = research area "Il Fuorn"; IS = imaging spectroscopy; NDVI = normalised difference vegetation index; NIR = near-infrared (spectral region between 760 and 1100 nm); NPV = non-photosynthetically active vegetation; PV = photosynthetically active vegetation; red = red part of the spectrum (spectral region between 600 and 760 nm); SI = spectral index; SNP = Swiss National Park; SR = simple ratio; TRU = research area "Val Trupchun"; wvl = wavelength.

Nomenclature
http://www.itis.gov/, http://www.theplantlist.org/

Received 20 May 2013
Accepted 6 June 2014
Co-ordinating Editor: Duccio Rocchini

Abstract

Aims: Imaging spectroscopy enables measurement of vegetation optical properties to predict vegetation characteristics that are important for a wide range of ecological applications. Our aim was to predict fresh above-ground biomass of heterogeneous alpine grasslands in two areas and at two ecological scales. We assessed model plausibility for an intensively studied alpine grassland site (plant community scale) having distinct biomass and ungulate grazing patterns.

Location: Alpine grasslands in the Swiss National Park.

Methods: Biomass data were collected in 51 plots and combined with imaging spectroscopy data to establish simple ratio models. We analysed the predictive power and transferability of models developed in two areas (Val Trupchun, Il Fuorn) and at two ecological scales (regional, local). In a next step, we compared our results to the broadband normalized difference vegetation index (NDVI). Finally, we assessed the correlations between model predictions and plant biomass distribution at the plant community scale.

Results: The best local simple ratio models yielded a model fit of $R^2 = 0.60$ and $R^2 = 0.30$, respectively, the best regional model a fit of $R^2 = 0.44$. NDVI model performance was weaker for the regional and one local area, but slightly better for the other local area. However, at the plant community scale only the local model showed a significant positive correlation ($R_S = 0.39$) with the known biomass distribution. Further, predictive power decreased when models were transferred from one local area to another or from one ecological scale to another.

Conclusions: Our study demonstrated that imaging spectroscopy is generally useful to predict above-ground plant biomass in alpine grasslands with distinct grazing patterns. Site-specific local models based on simple ratio indices performed better than the NDVI or regional models, suggesting that standardized approaches might not be adequate, particularly in heterogeneous grasslands inhabited by large ungulates. We emphasize the importance of collecting ground reference data covering the expected range of productivity and plant species composition. Moreover, plant community-scale data from a previous study proved to be extremely valuable to test model plausibility.

Schweiger, A.K. (*corresponding author, anna.schweiger@nationalpark.ch): Swiss National Park, Chaste Planta-Wildenberg, 7530 Zernez, Switzerland; Research Unit Community Ecology, Swiss Federal Institute for Forest, Snow and Landscape Research WSL, Zürcherstrasse 111, 8903 Birmensdorf, Switzerland; Remote Sensing Laboratories, Department of Geography, University of Zurich - Irchel, Winterthurerstrasse 190, 8057 Zürich, Switzerland &
Haller, R. (ruedi.haller@nationalpark.ch): Swiss National Park, Chastè Planta-Wildenberg, 7530 Zernez, Switzerland
Risch, A.C. (anita.risch@wsl.ch) &
Schütz, M. (martin.schuetz@wsl.ch): Research Unit Community Ecology, Swiss Federal Institute for Forest, Snow and Landscape Research WSL, Zürcherstrasse 111, 8903 Birmensdorf, Switzerland
Damm, A. (alexander.damm@geo.uzh.ch), **Kneubühler, M.** (mathias.kneubuehler@geo.uzh.ch) & **Schaepman, M.E.** (michael.schaepman@geo.uzh.ch): Department of Geography, Remote Sensing Laboratories, University of Zurich – Irchel, Winterthurerstrasse 190, 8057 Zürich, Switzerland

Doi: 10.1111/jvs.12214

Introduction

Grasslands are spatially and temporally heterogeneous landscape elements. The variability of topo-edaphic parameters creates spatial heterogeneity in soil (texture, moisture, nutrients; e.g. Frank et al. 1994; Turner et al. 1997) and plant properties (community composition, biomass; e.g. Lauenroth & Sala 1992; Knapp et al. 1993). Temporal heterogeneity in soil and plant properties is, in turn, largely related to seasonal and inter-annual variation in temperature and precipitation regimes (e.g. Lauenroth & Sala 1992; Epstein et al. 2002; Knapp et al. 2002). Besides these abiotic controls of spatio-temporal variability, herbivores can act as biotic drivers of grassland properties, as they have strong direct and indirect effects on ecosystem processes such as nutrient cycling or productivity (e.g. McNaughton 1979; McNaughton et al. 1997; Wardle et al. 2004; Risch & Frank 2006; De Knegt et al. 2008; De Jager & Pastor 2009). Thus, grassland ecosystems are particularly interesting for assessing interactions between environmental parameters, their impact on the heterogeneity and spatio-temporal variability of the vegetation and related activity of the herbivore community.

The spatio-temporal variability in the distribution of forage, i.e. nutritient quality or quantity of plant material, is important for understanding the behaviour of herbivores, since their activities are linked to specific spatial and temporal scales (Skidmore et al. 2010). Large ungulates show migration patterns and home range establishment at the regional or landscape scale, they choose suitable feeding areas and plant communities at the local scale, and select certain plant species or plant parts at the plant community scale (Senft et al. 1987). Consequently, predicting how vegetation quality and quantity varies in space and time is critical for understanding ungulate behaviour and is essential for wildlife conservation (Bailey et al. 1996; Ritchie & Olff 1999; Hebblewhite & Haydon 2010). As the amount and quality of vegetation in particular and ecosystem processes in general are, in turn, affected by herbivores, also plant–herbivore interactions change across both temporal and spatial scales (Bestelmeyer et al. 2011; Tanentzap & Coomes 2012; Zheng et al. 2012). Thus, spatially continuous information on vegetation characteristics at reasonable resolution covering large areas would be advantageous for comprehensively analysing plant–herbivore interactions, since different properties of ecological phenomena emerge when viewed at different scales (Skidmore & Ferwerda 2008).

In situ measurements of spatio-temporally heterogeneous grassland properties take considerable time and effort (Aplin 2005; Milton et al. 2009) and often conflict with the need to cover large areas (Ustin et al. 2004). Especially in mountainous regions, where the terrain is difficult to access, systematic *in situ* sampling of vegetation traits within traditional field campaigns is extremely laborious. If informative priors, e.g. considering physical factors such as soil properties, or radiation are readily available, extrapolations of vegetation traits from research plots to local scale may sometimes be possible. However, the extrapolation of findings from research plots usually suffers from uncertainties and knowledge gaps. Air- and space-borne remote sensing provide the only realistic mean to fill these gaps, by collecting spatially continuous information on environmental parameters over large areas (Kerr & Ostrovsky 2003; Aplin 2005).

In contrast to broadband sensors, such as Landsat with only a few spectral bands [four (Landsat 1–5) to eight bands (Landsat 8)], fine spatial resolution imaging spectroscopy (IS) offers the advantage of increased spectral sampling using 'hundreds' of spectral bands (Goetz et al. 1985). Thus, IS makes it possible to detect the radiometric response resulting from subtle changes in the composition of different land-cover types, typically soil or vegetation classes (Ustin et al. 2004; Aplin 2005; Wang et al. 2010). IS was successfully used to discriminate between plant functional types (e.g. Ustin & Gamon 2010; Schmidtlein et al. 2012), individual plant species (e.g. He et al. 2011), plant biochemical compositions (e.g. Skidmore et al. 2010; Youngentob et al. 2012) or available plant biomass (e.g. Mirik et al. 2005; Numata et al. 2008; Cho & Skidmore 2009), and thus has proven highly valuable for several fields of ecosystem research (Ustin et al. 2004; Goetz 2009; Schaepman et al. 2009).

The radiometric response (i.e. reflectance spectrum) of vegetation is determined by absorption and scattering of light, which is caused by chemical bonds and the three-dimensional structure of the plant and the canopy (Ustin et al. 2004). Specific regions of the spectrum known to be sensitive to these different biochemical or biophysical plant properties (see e.g. Curran 1989) can be combined to calculate spectral indices (SIs; Oldeland et al. 2010). For biomass estimation, numerous SIs have been developed during the past decades (for detailed descriptions and discussion of their properties see e.g. Broge & Leblanc 2001; Haboudane et al. 2004; Zarco-Tejada et al. 2005), with the most commonly used being the normalized difference vegetation index (NDVI; Rouse et al. 1974). SIs can be calculated using coarse (broadband) and fine (narrowband; i.e. IS) spectral resolution data. Broadband SIs, such as the broadband NDVI, are regularly used for comparing vegetation characteristics over large areas (e.g. on a global scale using satellite data) with constrained spatial detail. If information on vegetation characteristics is desired in complex landscapes (with variable percentages of vegetation cover, litter, woody elements and soil, etc.) and high

Doi: 10.1111/jvs.12214

spatial detail, narrowband SIs usually provide better results (Asner et al. 2000; Thenkabail et al. 2002). In combination with ground reference data narrowband SIs allow development of predictive models for vegetation characteristics specifically adapted to a study area. Although the importance of systematic ground sampling during satellite or aircraft over-flights was recognized decades ago (see e.g. Gamon et al. 1993), the lack of sufficient and high-quality ground reference plots (i.e. covering the expected variability) still often constrains the development of robust models and the implementation of validation and accuracy assessment (Lu 2006).

Generally, the relationship between grassland biomass and spectral indices holds best for moderate to short canopies that contain a high proportion of green, photosynthetically active material (Tucker 1979; Hill 2004). Estimating biomass in more complex, heterogeneous systems is much more challenging (Sims & Gamon 2002; Lu 2006; Cho & Skidmore 2009). Studies using satellite data investigated the possibility of spatial interpolation for predicting biomass (canopy to local scale; Numata et al. 2008), measuring the impact of herbivore grazing intensity (Todd et al. 1998; Numata et al. 2007) and assessing the influence of different plant species and canopy architecture on biomass prediction (Numata et al. 2008), but were carried out in managed rangelands with one or two dominant grass species. Similarly, airborne IS has been applied to predict variability in biomass patterns in arable land (e.g. Thenkabail et al. 2000; Hansen & Schjoerring 2003; Liu et al. 2010) and relatively uniform grasslands (Gamon et al. 1993). Comparatively few studies have used airborne IS to predict biomass in semi-natural grasslands (e.g. Mirik et al. 2005; Beeri et al. 2007; Cho et al. 2007; Cho & Skidmore 2009), and none of these studies tried to assess both plant biomass and the effects of plant–herbivore interactions within the same heterogeneous grassland ecosystem.

The goal of our study is to use airborne IS data to model vegetation quantity [total aboveground plant biomass (fresh weight; $g \cdot m^{-2}$)] in a highly heterogeneous alpine landscape, where three large ungulate species, red deer (*Cervus elaphus* L.), chamois (*Rupicapra rupicapra* L.) and ibex (*Capra ibex* L.), are ubiquitous and therefore strongly interact with the vegetation. More specifically, we used airborne IS data from the Airborne Prism Experiment (APEX; Jehle et al. 2010) and ground reference data to develop models for the prediction of biomass in alpine grasslands in two study areas [Val Trupchun (TRU) and Il Fuorn (FUO)] in the Swiss National Park (SNP). We analysed models developed at different ecological scales, i.e. the regional scale (entire SNP, ca. 170 km^2) and the local scale (TRU and FUO, ca. 22 and 30 km^2, respectively) and tested model transferability (1) between the regional and the local scale, and (2) between the two local scales. Further, we compared our results with a more standardized approach, the broadband NDVI. In addition, we tested our models on a small grassland site (Alp Stabelchod, plant community scale, ca. 11 ha) where additional field data for biomass were available (see Schütz et al. 2006; Thiel-Egenter et al. 2007).

It must be noted that the concept of scale can be viewed from a cartographic or an ecological perspective (Skidmore & Ferwerda 2008). While small scale in cartography means covering a large area in less detail (e.g. global maps of 1:1 000 000), small scale in ecology means covering a small area in great detail. We relate 'scale'the ecological hierarchy of large herbivore foraging. In this conceptual model scales are defined by the frequencies of switches within and between foraging patterns and the boundaries between scale units reflect the animals' behaviour (Senft et al. 1987). In the SNP, some individuals of the three ungulate species switch between regional scales during the course of their lifetimes, whereas practically all individuals change at the local scale several times per year. In contrast, the ungulates cross plant community boundaries usually several times per day. Since the three scales of our study (regional, local and plant community scale) relate to the way large ungulates interact with their environment, they are considered as ecologically meaningful subdivisions of the landscape continuum.

The results of this study, i.e. the assessment of a remote sensing-based approach to derive spatially continuous information on biomass in a complex alpine environment, will be used to facilitate the analysis of plant–herbivore interactions, which is one of the research priorities in the SNP (see Schütz et al. 2003, 2006; Risch et al. 2004, 2008, 2013; Suter et al. 2004; Thiel-Egenter et al. 2007; Spalinger et al. 2012).

Methods

Study area

The study was conducted in the SNP, located in southeast Switzerland. Elevation ranges from 1350 to 3170 m·a.s.l. The SNP encompasses an area of ca. 170 km^2. About 86 km^2 are covered by vegetation, with forests occupying 53 km^2 and grasslands 29 km^2. The average annual temperature is 0.9 ± 0.5 °C (mean ± SD), with a mean annual minimum of -18.8 ± 8.6 °C and a mean annual maximum of 13.6 ± 6.1 °C; mean annual precipitation is 744 ± 160 mm, with an annual minimum of 667 mm and an annual maximum of 1013 mm; mean daily wind speed is 5.3 ± 2.2 $km \cdot h^{-1}$, with hourly maxima of up to 29.2 $km \cdot h^{-1}$ and peak gusts of up to 100.8 $km \cdot h^{-1}$ (2008–2012, recorded at the park's weather station, Buffalora, at 1977 m·a.s.l.; MeteoSwiss 2013). The grasslands

in the SNP are characterized by a heterogeneous mosaic-like structure caused by small-scale microrelief variability resulting in variations in microclimate and soil properties. The heterogeneity is also reflected in high small-scale plant species richness: up to 40 plant species·m^{-2}. The plant growing season lasts from mid-May until mid-September. The SNP is known for its large populations of red deer, chamois and ibex, with densities of 9.6 red deer, 7.7 chamois and 1.7 ibex per km^2 (2010 population counts).

We selected two study areas within the SNP (regional scale) for developing local biomass models: TRU and FUO (Fig. 1). TRU is a southeast- to northwest-orientated valley that encompasses ca. 22 km^2; about 26% of the area is covered with grassland; bedrock consists of mainly limestone and calcareous schist. FUO extends over ca. 30 km^2 and consists of several side valleys; about 20% of the area is covered with grassland and the bedrock is mainly dolomite. Additionally, we used previously published biomass data from Alp Stabelchod (plant community scale), a grassland site of about 11 ha surrounded by forest and located in study area FUO (Fig. 1). Vegetation and soil properties, as well as the impact of large ungulates, on Alp Stabelchod have been studied intensively on a grid covering the entire site, with cells measuring 20 m × 20 m (Schütz et al. 2003, 2006; Thiel-Egenter et al. 2007).

Ground reference data: Regional and local scale

We established a total of 51 ground reference plots covering the entire range of exposures and elevations and the expected range of grassland biomass, plant species composition and grazing intensity. There were 25 plots in TRU, 26 in FUO (Fig. 2). We defined a minimum of 50 m × 50 m of grassland area for a ground reference plot to be established, and a minimum distance of 20 m between two plots. An individual plot was homogenous in species composition and cover and measured 6 m × 6 m to balance possible imprecision resulting from data processing. Plots did not contain large objects (trees, rocks, buildings) or trails, and were located at least 6 m from such objects. On 24 June 2010, just after IS data had been acquired (see below), we clipped the vegetation 1 cm above the ground on a 1 m × 1 m subplot in the centre of each plot (Fig. 2d). The vegetation was immediately sealed into plastic bags and weighed on the same day to determine fresh biomass. We then divided the ground reference data into three equal-sized groups differing in fresh biomass (low: 20.2–250.7 g·m^{-2}; medium: 250.7–443.3 g·m^{-2}; high: 443.3–1235.4 g·m^{-2}). From each group we randomly assigned half the data to the calibration and half to the validation data set (stratified random sampling).

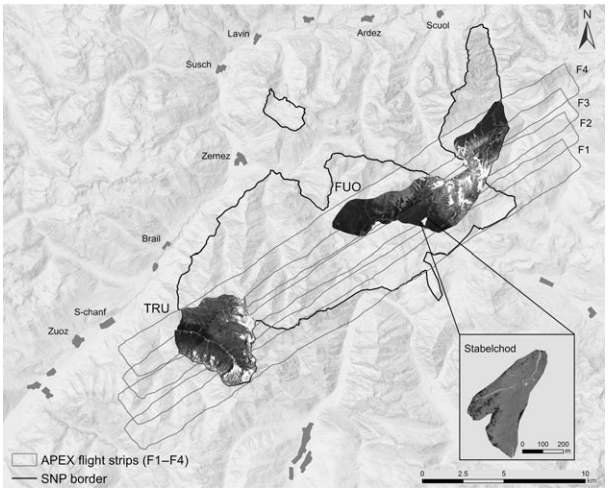

Fig. 1. Study areas Trupchun (TRU) and Il Fuorn (FUO) located within the Swiss National Park (SNP). Four APEX flight strips (F1, F2, F3, F4) were included in our study. The enlargement in the lower right corner shows Alp Stabelchod.

Ground reference data: Plant community scale

Spatially continuous biomass data at the plant community scale are particularly important for the investigation of plant–herbivore interactions. Therefore, we additionally obtained ground reference data for Alp Stabelchod from two previously published data sets to assess model plausibility. One data set contained information on soil phosphorus (soil P) as well as the proportion of total cover of the two main vegetation types found on Alp Stabelchod (short- and tall-grass vegetation) measured in a 20 m × 20-m grid covering the entire grassland (Schütz et al. 2006). The second contained grassland above-ground net primary productivity (ANPP g dry weight·m^{-2}) and biomass (g dry weight·m^{-2}) data from an exclosure experiment. The exclosures were located along soil P gradients in both vegetation types on selected 20 m × 20-m grid cells (Schütz et al. 2006; Thiel-Egenter et al. 2007). In the first step, these data were used to calculate plant biomass for each grid cell. As plant biomass was independent of soil P regardless of vegetation type (Thiel-Egenter et al. 2007), average plant biomass per grid cell was calculated by multiplying the total proportion of short-grass vegetation per grid cell with the average value for short-grass biomass (14.81 g·dry weight·m^{-2}) and adding the proportion of tall-grass cover multiplied by the average value for tall-grass biomass (110.9 g·dry weight·m^{-2}). In a second step, ANPP and biomass consumption by ungulates was calculated at the same scale. As ANPP was independent of soil P for short-grass (103.3 g·dry weight·m^{-2}), but depended on soil P in tall-grass (Thiel-Egenter et al.

Doi: 10.1111/jvs.12214

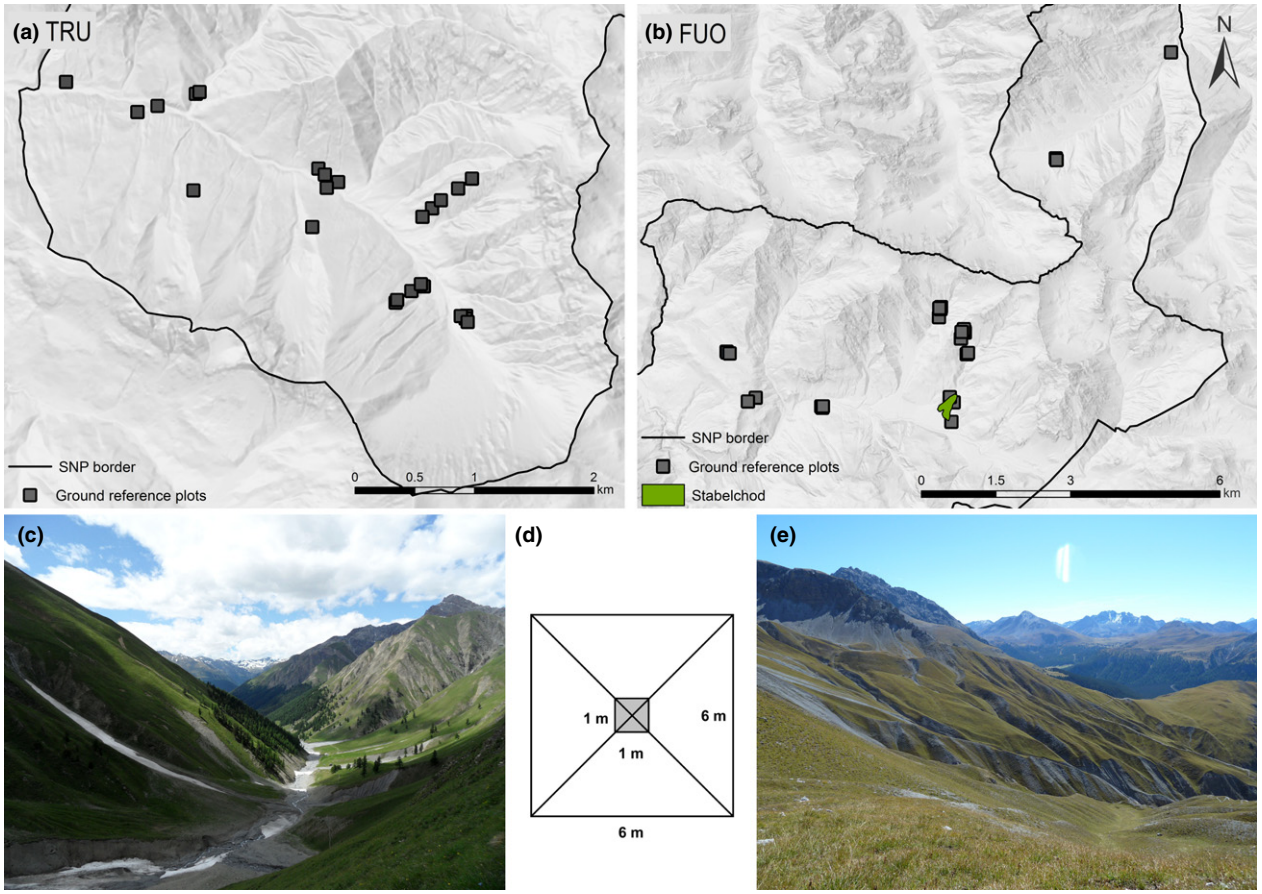

Fig. 2. Maps and photos of the study areas TRU (**a**, **c**) and FUO (**b**, **e**), respectively, and design of the ground reference plots (**d**).

2007) vegetation, tall-grass ANPP (ANPP_t) was calculated for each grid cell separately using equation (1).

$$\text{ANPP\_t}(\text{g dry weight} \cdot \text{m}^{-2}) = 0.67^{*}\text{soil}P + 3.29 \quad (1)$$

.

Average ANPP per grid cell was then calculated using the total proportion of short- and tall-grass cover per grid cell as described for plant biomass. Biomass consumption by ungulates (g·dry weight·m^{-2}) was calculated for each grid cell by subtracting plant biomass from ANPP and converted to percentage (%).

Imaging spectroscopy data

Imaging spectroscopy data were collected under cloud-free conditions on 24 June 2010 between 11:29 and 12:06 h Central European summer time (CEST) using the airborne imaging spectrometer APEX (Jehle et al. 2010). The sun zenith angle was between 31.8° and 28.1°, the sun azimuth between 127.5° and 139.1°, and the mean flight altitude per flight line was between 6665 and 6667 m·a.s.l. APEX is a dispersive push broom sensor, mounted on a Dornier DO-228 aircraft operated by Deutsches Zentrum für Luft- und Raumfahrt (DLR, German Aerospace Centre), and covers the wavelength region from 380 to 2500 nm in 312 contiguous spectral bands with a full width at half maximum (FWHM) ranging from 4 to 12 nm. We used 301 bands for our analysis after removing noisy bands. The spatial sampling interval across track (ground resolution) depends on the flight altitude above ground level (AGL) and is between 1.75 m at 3500 m AGL and 2.5 m at 5230 m AGL. Therefore, the ground pixel size was resampled to 2 m × 2 m using a nearest neighbour interpolation (for more details see Schläpfer & Richter 2002). Measured raw digital numbers (DN) of the four flight lines (Fig. 1) were converted to radiances by applying calibration coefficients obtained from an after-flight calibration campaign (Jehle et al. 2010). Calibrated radiance data were then geometrically corrected using a parametric geo-rectification approach implemented in the PARGE software package (Schläpfer & Richter 2002). Surface reflectances, more specifically, hemispheric conical reflectance factors (HCRF; see Schaepman-Strub et al.

Doi: 10.1111/jvs.12214

2006) were retrieved from at-sensor radiance data by applying a physically based atmospheric correction approach as implemented in the ATCOR-4 software (Richter & Schläpfer 2002). ATCOR-4 uses the atmospheric radiative transfer model MODTRAN to describe atmospheric absorption and scattering processes and to compensate for their respective impact on the measured at-sensor radiance signals. Parameters describing the atmospheric status required by MODTRAN were set to realistic values (e.g. CO_2 level was set to 380 ppm), while others like aerosol optical depth or atmospheric water vapour were retrieved pixel-wise from the image data itself. The aerosol size and distribution was approximated with the a-priori defined models 'mid-latitudinal summer' and 'rural atmosphere'. Geometric mis-registration of the orthorectified data was evaluated using ground-based differential global positioning system (DGPS) measurements, and was found to be less than one pixel (±2 m) in flat terrain and up to two pixels (±4 m) on steep slopes (Damm et al. 2012). In cases where reference plots were covered twice by APEX (overlapping flight lines), both flight lines were used as input for modelling. The two measurements can be considered independent due to reflectance anisotropy effects (caused by differing times of day, flight angles, flight heights, etc.) and are assumed to make our models more robust. Consequently, we had 43 observations for TRU (22 calibration; 21 validation) and 41 observations for FUO (21 calibration; 20 validation).

Model building and mapping

The spectral properties of vegetation are determined by their chemical composition (e.g. pigment concentration, water content), structure (leaf internal and external structure) and the spatial arrangement of these structures (Tucker 1979; Ustin et al. 2004; Jones & Vaughan 2010; Wang et al. 2010). Three spectral regions are of primary interest for plant biomass assessment (Tucker 1979; Horler et al. 1983; Myneni et al. 1995; Thenkabail et al. 2002): the red (600–760 nm), near-infrared (NIR; 760–1100 nm) and red edge (transition zone between 640 and 760 nm). The more chlorophyll contained in the vegetation the higher the absorption in the red (Tucker 1977; Myneni et al. 1995), while a more complex leaf and canopy structure results in more scattering and less absorption in the NIR (Tucker 1979; Curran et al. 1991). The red edge is defined as the sharp increase in reflectance between these two regions (Horler et al. 1983) and thus marks the boundary between chlorophyll absorption and volume scattering (Curran et al. 1991; Jones & Vaughan 2010).

Both the calibration plots from TRU and FUO (43 data points) were used to calculate a model valid for the entire SNP (regional model). As the plots measured 6 m × 6 m and the pixel size of the IS data was 2 m × 2 m, a 3 × 3 pixel aggregation was defined to extract the reflectance measurements from the IS data and to calculate the average reflectance of all nine aggregated pixels per plot. To test for boundary effects, we also calculated the average reflectance over 25 aggregated pixels (5 × 5 pixel aggregations), and found no significant differences between the two (results not shown). This confirms that our ground reference plots were located in homogenous areas on a scale of at least 10 m × 10 m. We then calculated all simple ratios (SR = band j/band i) per nine aggregated pixels per plot for the band combinations located in the spectral regions described above: band j was located in the NIR (760–1098 nm; band 76–125) and band i in the red part of the spectrum (598–756 nm; band 29–75), resulting in a total of 2350 combinations. All SRs of the calibration plots were afterwards used as input to model fresh biomass ($g \cdot m^{-2}$) with linear, exponential and second-order polynomial functions. Exponential and second-order polynomial functions were used to account for potential sources of interference, such as fractions of different vegetation types, surface heterogeneity or topographic effects. The best model was selected using Akaike's information criterion (AIC) and applied to predict fresh biomass for the entire SNP (both TRU and FUO validation data). Model validation was performed using bootstrapping with 100 replications. We evaluated model fit and predictive accuracy by calculating the coefficient of determination ($R^2 \pm$ SD) and the root mean square error (RMSE ± SD). Additionally, we assessed the performance of the regional model (SNP) when used to estimate fresh biomass at the two local scales. Therefore, the best SNP model was validated separately for TRU (using TRU validation data only; thereafter named SNP_TRU) and FUO (using FUO validation data only; SNP_FUO), and model fit and predictive accuracy were calculated.

In a next step, the same method was used to calibrate two local models TRU and FUO separately, using only the TRU and FUO calibration data. The best models were again validated for each study area using the bootstrapping approach, and model fit and predictive accuracy were calculated. To assess whether a specific local SR could be used to predict fresh biomass of another local area, the best SR selected for FUO was used to calibrate a model for TRU (using TRU calibration data only; thereafter named FUO_TRU) and the best SR selected for TRU was used to calibrate a model for FUO (using FUO calibration data only; TRU_FUO). Again, the corresponding validation data sets were used for model validation with bootstrapping, and model fit and predictive accuracy were calculated. We refer below to these models (FUO_TRU and TRU_FUO) as the transferred local models.

Doi: 10.1111/jvs.12214

In addition, we simulated broadband NDVI to compare our best regional (SNP) and local models (TRU, FUO) with a more standardized approach. Therefore, we calculated the mean reflectance of all APEX bands in the red (630.5–690.0 nm) and NIR (760.4–898.1 nm), corresponding to Landsat Thematic Mapper (TM) band 3 and band 4 (i.e. 630–690 and 760–900 nm, respectively) and calculated broadband NDVI (NDVI = NIR − red/NIR + red). Next, we fitted linear models for biomass against the simulated broadband NDVI for the entire SNP and the local areas TRU and FUO separately, using the corresponding calibration data sets. As before, we used bootstrapping to validate the models for each study area and calculated model fit and predictive accuracy.

Finally, we assessed if our regional, local, transferred local and NDVI models succeeded in predicting biomass at the plant community scale on Alp Stabelchod, an intensively studied grassland site with known biomass and consumption rates. Pixel size of the IS data used for the regional and local models was 2 m × 2 m, whereas the grid on Alp Stabelchod measured 20 m × 20 m. Therefore, the mean predicted biomass was calculated for the 100 2 m × 2 m pixels corresponding to each grid cell using the regional (SNP), local (FUO), transferred local (TRU_FUO) and NDVI (NDVI_FUO) model. We calculated the correlation coefficient between biomass at the plant community scale (see method section: Ground reference data: Plant community scale) and predicted biomass from our models to assess which of the models best depicted the pattern. For this purpose, either Pearson's correlation coefficient (R) or Spearman's rank correlation coefficient (R_S) was used, depending on whether the biomass data met the normality and homogeneity criteria.

Since our models were designed to predict only the biomass of grasslands, we applied linear spectral unmixing (LSU) to exclude areas dominated by forest, rock, snow or water from mapping (Roberts et al. 1993). Imaging spectroscopy data were prepared using ENVI (v 4.7; Exelis Visual Information Solutions, Boulder, CO, US). For modelling, we used R (v 2.15.1; R Foundation for Statistical Computing, Vienna, AT), for spatial data handling and mapping, ArcGIS (v 10.0; Environmental Systems Research Institute, Redlands, CA, US).

Results

Fresh weights of above-ground biomass on our 51 ground reference plots ranged from 20.2 to 1235.4 $g \cdot m^{-2}$ (354.7 ± 241.7 $g \cdot m^{-2}$; mean ± SD). For the 25 TRU plots mean biomass was 400.1 ± 265.3 $g \cdot m^{-2}$ (range 37.2–1235.4 $g \cdot m^{-2}$), for the 26 FUO plots mean biomass was 311.1 ± 212.8 $g \cdot m^{-2}$ (range 20.2–862.1 $g \cdot m^{-2}$).

The performance of the best regional model (SNP; Fig. 3a) was moderate. However, the broadband NDVI model (NDVI_SNP; Fig. 3b) was considerably weaker, both in terms of R^2 and RMSE.

In area TRU, the site-specific local model (TRU; Fig. 4a) yielded the best fit of all models. The transferred local model (FUO_TRU; Fig. 4b), the regional model applied to this local scale (SNP_TRU; Fig. 4c) and the broadband NDVI model (NDVI_TRU; Fig. 4d) all clearly performed less well. However, when model predictions were mapped for TRU, similar patterns in terms of the high and low biomass became evident (Fig. 5). In area FUO, the site-specific local model (FUO; Fig. 6a) performed moderately. The transferred local model (TRU_FUO; Fig. 6b) was slightly weaker, the regional model applied to this local scale (SNP_FUO; Fig. 6c) and the broadband NDVI model (NDVI_FUO; Fig. 6d) performed slightly better, both in terms of R^2 and RMSE.

Most interestingly, only the site-specific local model (FUO) correctly predicted the known biomass pattern on Alp Stabelchod (compare Fig. 7a–d with Fig. 8a). Previously published data from Alp Stabelchod show high biomass in the western part (Fig. 8a), while high consumption rates of ungulates lead to low biomass in the eastern part of the meadow (Fig. 8b). A similar pattern was predicted with the site-specific local model (FUO; Fig. 7a), whereas both the regional (SNP_FUO; Fig. 7c) and the broadband NDVI (NDVI_FUO; Fig. 7d) model predicted the opposite. Predictions of the transferred local model (TRU_FUO; Fig. 7b) showed an intermediate prediction, featuring no clear differences between the western and eastern parts of the meadow. Correlation analyses revealed that the biomass pattern was, indeed, only correctly reflected in the site-specific local model, as we found a positive correlation between measured biomass at the plant community scale and predicted biomass from the model (FUO: $R_S = 0.39$, $P < 0.01$). A negative correlation between measured and predicted biomass was found for the regional (SNP_FUO: $R = -0.44$, $P < 0.01$) and the broadband NDVI (NDVI_FUO: $R_S = -0.43$, $P < 0.01$) model, and a non-significant one for the transferred local model (TRU_FUO: $R_S = -0.14$, $P = 0.10$).

Discussion

Suitability of selected vegetation indices

The simple ratio indices used in this study depended, by definition, on chlorophyll absorption in the red and volume scattering in the NIR part of the spectrum (Myneni et al. 1995; Asner 1998; Jones & Vaughan 2010). Both spectral regions are regularly and successfully used for predicting plant biomass (e.g. Tucker 1979; Mirik et al. 2005; Beeri et al. 2007; Cho et al. 2007; Fava et al. 2009). Model

Doi: 10.1111/jvs.12214

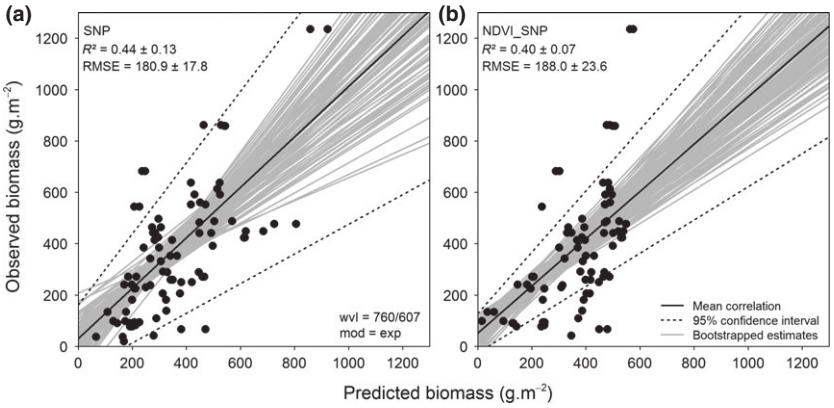

Fig. 3. Best regional model (SNP; **a**) and broadband NDVI model (NDVI_SNP; **b**) predicting fresh biomass at the regional scale. Coefficients of determination ($R^2 \pm$ SD), root mean square errors of prediction (RMSE $\pm$ SD), wavelengths (wvl) for bands j and i in nm and model type (mod, exp = exponential) are indicated.

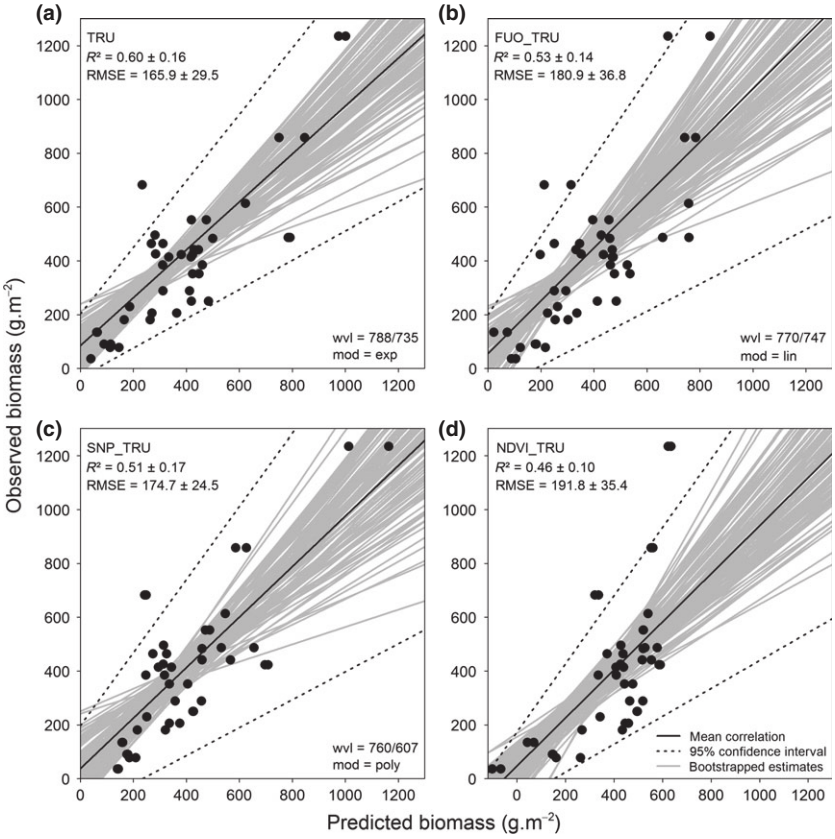

Fig. 4. Best local model (TRU; **a**), transferred local (FUO_TRU; **b**), regional (SNP_TRU; **c**) and broadband NDVI (NDVI_TRU; **d**) model predicting fresh biomass at the local scale TRU. Coefficients of determination ($R^2 \pm$ SD), root mean square errors of prediction (RMSE $\pm$ SD), wavelengths (wvl) for bands j and i in nm and model type (mod, lin = linear, exp = exponential, poly = polynomial) are indicated.

fit of the SNP and TRU models (R^2 of 0.44 $\pm$ 0.13 and 0.60 $\pm$ 0.16, respectively) were in the range of other studies estimating biomass in semi-natural grasslands using airborne IS data. The fit of the FUO model (R^2 of 0.30 $\pm$ 0.10) was weaker. Cho et al. (2007) and Cho & Skidmore (2009) reported R^2 values of 0.53, 0.56 and 0.64 for biomass estimation in the Italian Apennines, while Beeri et al. (2007) and Mirik et al. (2005) indicated R^2

Doi: 10.1111/jvs.12214

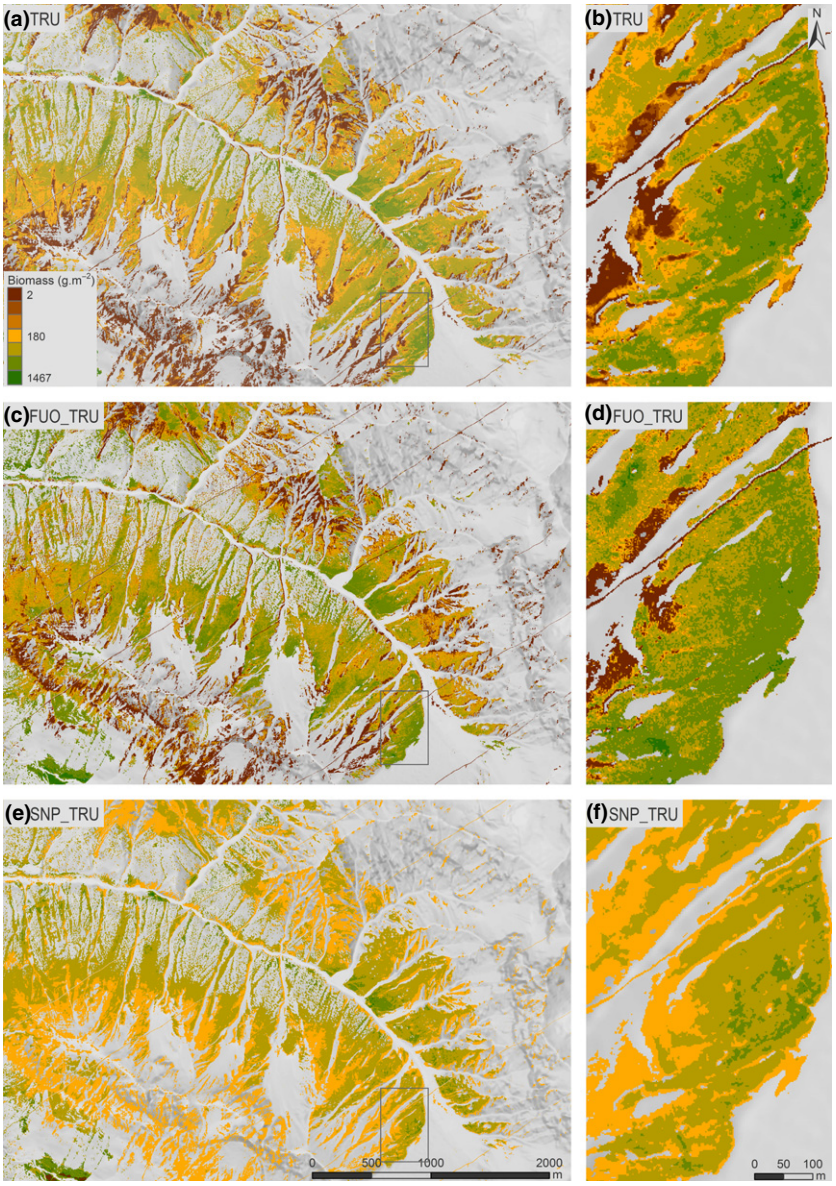

Fig. 5. Biomass (fresh weight) mapped for TRU using the best local model (TRU; **a**, **b**), the transferred local (FUO_TRU; **c**, **d**) and the regional (SNP_TRU; **e**, **f**) model.

values of 0.73 and 0.87 for biomass estimation in the prairies of North Dakota and Wyoming, respectively. The RMSE value of the TRU model (RMSE = 165.9 ± 29.5 g·m^{-2}) was only slightly higher than the values between 97.6 and 144.7 g·m^{-2} of Beeri et al. (2007). Again, the predictive accuracy of the FUO model (RMSE = 193.9 ± 33.7 g·m^{-2}) was lower. In our opinion, there are several reasons why biomass prediction in study area FUO was more challenging than in TRU. First, the range of biomass values in FUO (20.2−862.1 g·m^{-2}) was lower than in TRU (37.2−1235.4 g·m^{-2}). Generally, the trade-off between the range of model parameters and measurement errors leads to model fit becoming weaker when the range of values is comparatively low and measurement errors are high (as is naturally the case when sampling biomass in the field). Additionally, when classifying slope and aspect based on a 2 m × 2 m digital elevation model (DEM) using six classes for slope (<10%–20%–30%–40%–50%–>50%) and eight classes for exposure (N-NO-O-SO-S-SW-W-NW), FUO proved to be more variable than TRU. In study area FUO the four middle classes for slope contained between 11% and 31% of all raster cells and the classes <10% and >50% contained each more than 5%, while in area TRU 67% of all raster cells fell

Doi: 10.1111/jvs.12214

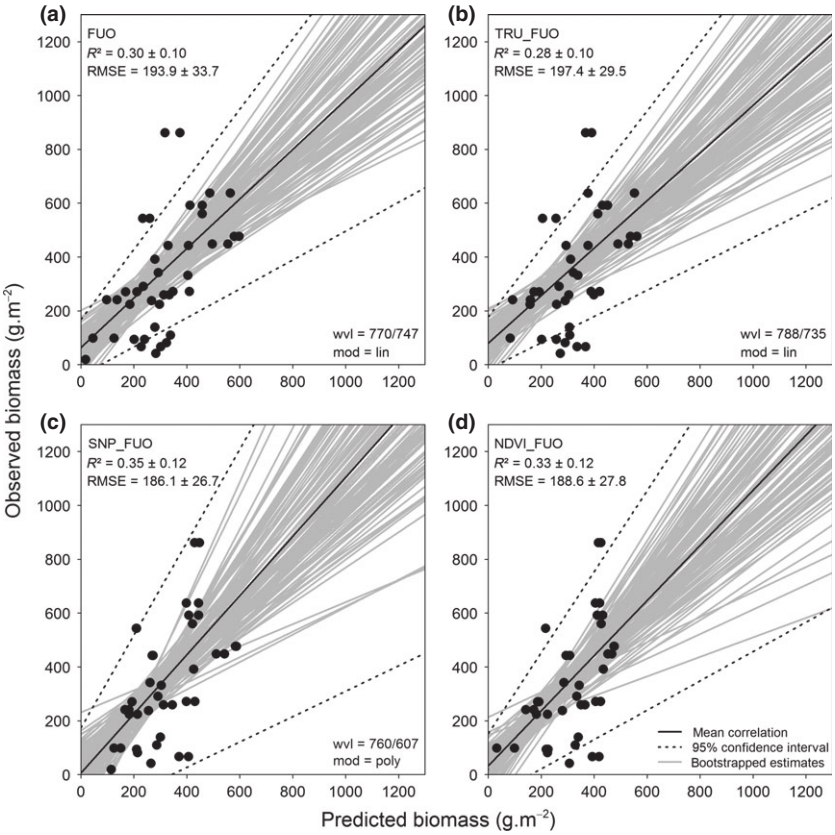

Fig. 6. Best local model (FUO; **a**), transferred local (TRU_FUO; **b**), regional (SNP_FUO; **c**) and broadband NDVI (NDVI_FUO; **d**) model predicting fresh biomass at the local scale FUO. Coefficients of determination ($R^2 \pm$ SD), root mean square errors of prediction (RMSE $\pm$ SD), wavelengths (wvl) for bands j and i in nm and model type (mod, lin = linear, poly = polynomial) are indicated.

in the classes between 30% and 50%. Similarly, all exposure classes in the area FUO contained between 8% and 17% of all raster cells, whereas in area TRU more than 70% of all raster cells were exposed to either N-NO or S-SW. Although topographic variation was minimized using ATCOR (slope and aspect correction for irradiance at the surface), greater topographic variability in area FUO could have negatively influenced model performance. Moreover, TRU featured a higher proportion of grasslands compared to FUO (26% vs 20%) and the grassland patches in TRU were larger and less fragmented. Consequently, scattering effects emerging from boundaries between adjacent grasslands and forest or between grassland and rocks (Jiang et al. 2012) probably had a greater influence in FUO. Differences in soil reflectance are also assumed to play a role in FUO, where grassland vegetation cover at the small scale was somewhat less than 100%, while it was almost always 100% or more in TRU. Probably the most important factor influencing model performance in FUO was the high amount of non-photosynthetically active vegetation (NPV) caused by distinct grazing patterns, as we discuss in more detail below. While Cho et al. (2007) and Cho & Skidmore (2009) estimated photosynthetically active vegetation (PV) only, and Beeri et al. (2007) conducted their study in rangeland where a lower amount of more evenly distributed NPV is expected, up to 50% NPV was found in one vegetation type in area FUO (M. Schütz, unpubl. data).

Interestingly, only the site-specific local model FUO correctly reproduced the known biomass pattern at Alp Stabelchod, although both standardized approaches (i.e. the regional SNP_FUO model and the NDVI_FUO model) indicated better model fit. This suggests that standardized approaches might not provide the ideal solution for predicting biomass patterns, particularly in heterogeneous landscapes with distinct vegetation and grazing patterns. It has been shown that IS is able to detect subtle changes in narrowband absorption features (Ustin et al. 2004; Aplin 2005; Wang et al. 2010) that are only partially approachable using broadband spectral information (Asner 1998). For example, narrow bands in the red part of the spectrum have proven to be much more sensitive to differences in chlorophyll content (Carter 1998; Jones & Vaughan 2010), a pattern that cannot be fully detected using broad bands

Doi: 10.1111/jvs.12214

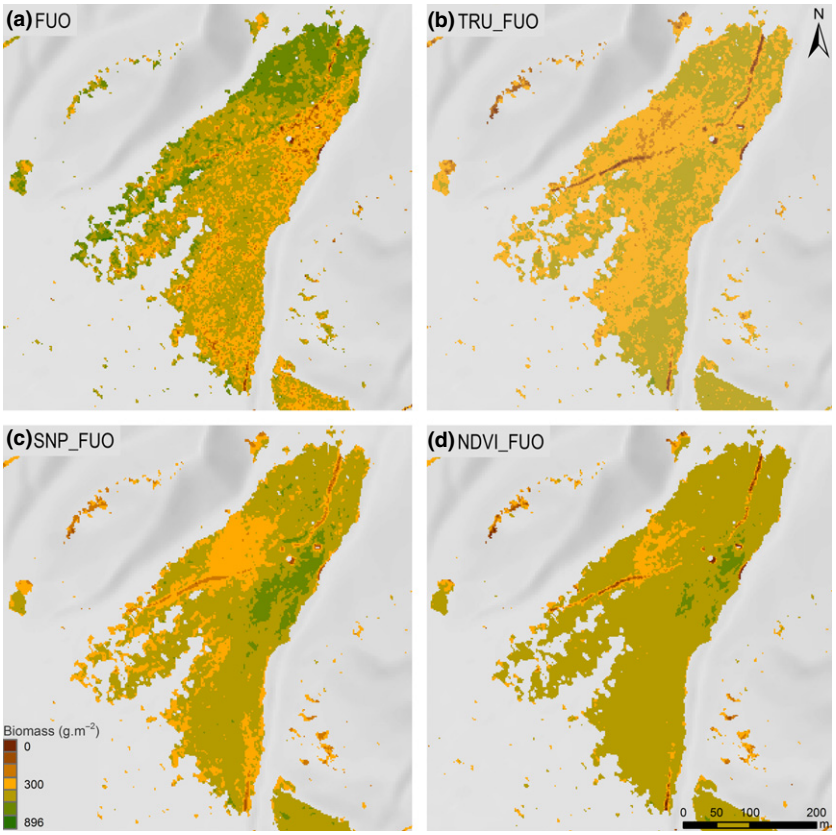

Fig. 7. Biomass (fresh weight) mapped at the plant community scale (Alp Stabelchod) using the best local model (FUO; **a**), the transferred local (TRU_FUO; **b**), the regional (SNP_FUO; **c**) and the broadband NDVI (NDVI_FUO; **d**) model.

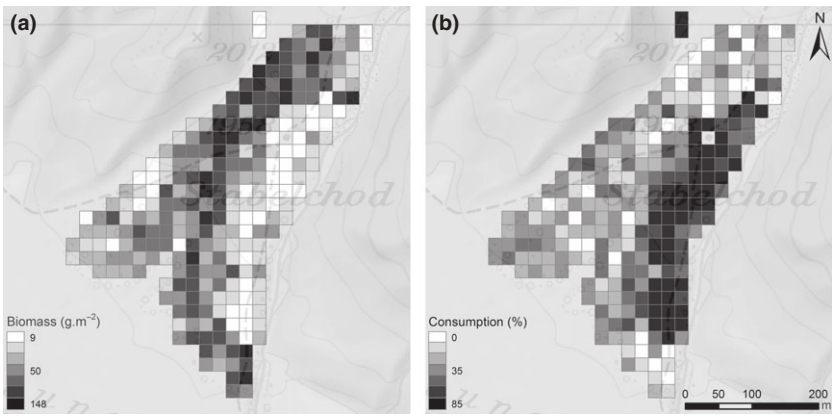

Fig. 8. Biomass (dry weight; **a**) and biomass consumption (**b**) mapped at the plant community scale (Alp Stabelchod) using data from Schütz et al. (2006) and Thiel-Egenter et al. (2007).

(Curran 1994). Additionally, broadband SIs can be unstable, varying with soil colour, canopy structure, leaf optical properties and atmospheric conditions (Huete & Jackson 1988; Middleton 1991; Todd et al. 1998). However, site and sensor specificity is not only a characteristic of broadband SIs, but of statistical models in general, which makes them unsuitable for application in large areas or different seasons/scales (e.g. Curran 1994; Gobron 1997; Cho & Skidmore 2009). Therefore, it was not surprising that our local models performed better than the regional models, but were not transferable between sites and scales, as they are highly parameterized for the specific study areas. How-

Doi: 10.1111/jvs.12214

ever, while our models are not transferable, our method – selecting the best site-specific SR index – can also be used in other study areas and seems to be advantageous in heterogeneous grasslands with distinct grazing patterns.

Biomass estimation in a heterogeneous landscape grazed by large ungulates

Biomass estimation using IS data in diverse and heterogeneous communities is challenging (Lu 2006; Cho & Skidmore 2009), since chemical composition and canopy structure is known to vary within and between plant species (Wright et al. 2001; Westoby et al. 2002). Having, in addition, large ungulates grazing on heterogeneous grasslands makes biomass estimation even more complicated, as ungulates are known to alter plant growth and resource allocation (McNaughton 1979; McNaughton et al. 1997; Schütz et al. 2006; Risch et al. 2007; Frank et al. 2011) and therefore the composition and structure of vegetation (Collins et al. 1998; Schütz et al. 2003; Risch & Frank 2006; Numata et al. 2007).

The interaction between ungulate grazing and vegetation community structure can be illustrated for Alp Stabelchod, a grassland site within study area FUO. The vegetation of the eastern part of Alp Stabelchod has been shown to be more nutrient-rich compared to the western part due to differences in former land use (for more details see Schütz et al. 2006). Therefore, large ungulates graze much more intensively (around 60% consumption) on the eastern compared to the western part of the site (around 16% consumption; cf. Schütz et al. 2006). As a consequence of differences in soil nutrient concentrations and grazing intensity, very short (grazed down to 2 cm) but nutrient-rich vegetation containing high levels of chlorophyll predominates in the eastern part of Alp Stabelchod. The dominating plant species are grasses, mainly *Festuca rubra* L. and *Briza media* L., and total NPV (senescent grass, litter) is <5% (M. Schütz, unpubl. data). On the western part of Alp Stabelchod, poorer soils resulted in lower plant quality and therefore lower grazing pressure (higher vegetation; around 20 cm). The dominating plant species is the sedge *Carex sempervirens* Vill., and 30% to 50% of plant material in this vegetation type is NPV (M. Schütz, unpubl. data).

Even small amounts of NPV can mask the spectral response in the red part of the spectrum (Roberts et al. 1993; Asner 1998; Beeri et al. 2007; Numata et al. 2007) and lead to underestimation of biomass in NPV-rich communities (He et al. 2006; Beeri et al. 2007; Verrelst et al. 2010). Asner (1998) found that a NPV content of 10% almost doubles, a NPV content of 20% triples and a NPV content of 50% causes a six-fold increase in grassland canopy reflectance in the red part of the spectrum. Additionally, since our SR indices depended on the greenness of the vegetation (Tucker 1979; Cohen & Goward 2004), biomass in the chlorophyll-rich short-grass might have been overestimated by the regional (SNP_FUO), transferred local (TRU_FUO) and NDVI (NDVI_FUO) model. Model improvements might be achievable when separating NPV from PV and introducing an empirical canopy greenness factor (Gamon et al. 1993) or modelling PV only, as done in other studies (He et al. 2006; Beeri et al. 2007; Boschetti et al. 2007). However, in our opinion including both NPV and PV for estimating biomass is important, since both contribute to biogeochemical cycling and are essential components of ecosystem functioning (Beeri et al. 2007). For grazed systems, Numata et al. (2008) suggested sorting NPV from PV after clipping the biomass in the field and combining two separate indices, one for NPV and one for PV. However, this approach would be extremely laborious since single grass leaves are often composed of both dead and living parts that would need to be separated. A less time-consuming approach would be spectral unmixing to determine the proportion of NPV and PV per pixel (see e.g. Gamon et al. 1993; Roberts et al. 1993; Asner & Heidebrecht 2002; Numata et al. 2007). However, both endmembers, PV and NPV, produce volume scattering, which generates ambiguities in the unmixing process. Thus, a non-linear unmixing approach would be most appropriate here. This would require additional field spectrometer measurements, since the spatial resolution of APEX is too coarse to collect pure pixels from the image when the vegetation is highly heterogeneous and mosaic-like (as in our case). Nevertheless, it would be worth testing this approach in a future study. The differences in vegetation communities and NPV distribution between heavily and lightly grazed areas were expected to be less distinct in TRU, which additionally explains why the TRU models had higher predictive power. As more forage is available in this area (TRU: 400.1 ± 265.3 g·m^{-2} (mean ± SD); FUO: 311.1 ± 212.8 g·m^{-2}), grazing is more evenly distributed. Therefore, overall grazing pressure is lower and grazers do not increase vegetation heterogeneity as much as in FUO.

The challenge in applying satellite or aircraft images to ecological studies lies in relating spectral and spatial information in an image to the vegetation pattern and processes on the ground (Gamon et al. 1993). Although some improvement through the application of different modelling techniques (e.g. spectral unmixing) might be possible, the fact that the local FUO model correctly predicted the biomass pattern on Alp Stabelchod known from previous studies was thus a success. Recalling the high predictive accuracy of the TRU model, we are confident that our sampling design covered vegetation heterogeneity within both local areas, and that our site-specific local models are

Doi: 10.1111/jvs.12214

suited as baseline data for detailed analysis of plant–herbivore interactions.

Conclusions

Our study shows that fine spatial resolution imaging spectroscopy can be successfully used to predict fresh aboveground biomass in a highly heterogeneous alpine landscape with distinct grazing patterns. More specifically, our site-specific local models based on SR indices performed better than regional or NDVI models, suggesting that standardized approaches might not always provide the best solution for predicting biomass in challenging landscapes. However, when following our modelling approach, two issues should be considered: first, since statistical models are highly site- and sensor-specific (Curran 1994; Gobron 1997), attention should be given to understanding the applicable scale defined by the characteristics of input data to the original model (Lu 2006). As demonstrated in our study, statistical models developed for one study site should not be transferred to another or used to predict patterns at other scales without checking for plausibility. For this purpose, independent data, ideally sampled on a continuous, relatively fine grid, are highly advantageous. Second, since the availability of sufficient and high-quality ground reference plots often limits the development of robust biomass models and the validation of the results (Lu 2006), a sampling design covering the entire expected range of biomass and heterogeneity should be used. If the distribution of NPV and PV is uneven, separating NPV from PV in the modelling phase should be considered.

Acknowledgements

The study was supported by the Swiss National Park. APEX data collection and processing was supported by a grant of the Swiss University Conference and ETH-Board in the framework of the HyperSwissNet project and the Scientific Council of the Swiss National Park. We thank Dominik Affolter, Rolf Bösch, Martin Brüllhardt, Antonia Eisenhut, Alan Haynes, Miriam Herrmann, Melanie Hodel, Ulrich Kias and Mirjam von Rütte for assistance in the field; Christian Schmid for survey and GIS support; Alan Haynes and Maia Rapp for modelling support; and Pia Anderwald for proofreading the manuscript.

References

Aplin, P. 2005. Remote sensing: ecology. *Progress in Physical Geography* 29: 104–113.

Asner, G.P. 1998. Biophysical and biochemical sources of variability in canopy reflectance. *Remote Sensing of Environment* 64: 234–253.

Asner, G.P. & Heidebrecht, K.B. 2002. Spectral unmixing of vegetation, soil and dry carbon cover in arid regions: comparing multispectral and hyperspectral observations. *International Journal of Remote Sensing* 23: 3939–3958.

Asner, G.P., Wessman, C.A., Bateson, C.A. & Privette, J.L. 2000. Impact of tissue, canopy, and landscape factors on the hyperspectral reflectance variability of arid ecosystems. *Remote Sensing of Environment* 74: 69–84.

Bailey, D.W., Gross, J.E., Laca, E.A., Rittenhouse, L.R., Coughenour, M.B., Swift, D.M. & Sims, P.L. 1996. Mechanisms that result in large herbivore grazing distribution patterns. *Journal of Range Management* 49: 386–400.

Beeri, O., Phillips, R., Hendrickson, J., Frank, A.B. & Kronberg, S. 2007. Estimating forage quantity and quality using aerial hyperspectral imagery for northern mixed-grass prairie. *Remote Sensing of Environment* 110: 216–225.

Bestelmeyer, B.T., Goolsby, D.P. & Archer, S.R. 2011. Spatial perspectives in state-and-transition models: a missing link to land management? *Journal of Applied Ecology* 48: 746–757.

Boschetti, M., Bocchi, S. & Brivio, P.A. 2007. Assessment of pasture production in the Italian Alps using spectrometric and remote sensing information. *Agriculture, Ecosystems and Environment* 118: 267–272.

Broge, N.H. & Leblanc, E. 2001. Comparing prediction power and stability of broadband and hyperspectral vegetation indices for estimation of green leaf area index and canopy chlorophyll density. *Remote Sensing of Environment* 76: 156–172.

Carter, G.A. 1998. Reflectance wavebands and indices for remote estimation of photosynthesis and stomatal conductance in pine canopies. *Remote Sensing of Environment* 63: 61–72.

Cho, M.A. & Skidmore, A.K. 2009. Hyperspectral predictors for monitoring biomass production in Mediterranean mountain grasslands: Majella National Park, Italy. *International Journal of Remote Sensing* 30: 499–515.

Cho, M.A., Skidmore, A., Corsi, F., Van Wieren, S.E. & Sobhan, I. 2007. Estimation of green grass/herb biomass from airborne hyperspectral imagery using spectral indices and partial least squares regression. *International Journal of Applied Earth Observation and Geoinformation* 9: 414–424.

Cohen, W.B. & Goward, S.N. 2004. Landsat's role in ecological applications of remote sensing. *BioScience* 54: 535–545.

Collins, S.L., Knapp, A.K., Briggs, J.M., Blair, J.M. & Steinauer, E.M. 1998. Modulation of diversity by grazing and mowing in native tallgrass prairie. *Science* 280: 745–747.

Curran, P.J. 1989. Remote sensing of foliar chemistry. *Remote Sensing of Environment* 30: 271–278.

Curran, P.J. 1994. Imaging spectrometry. *Progress in Physical Geography* 18: 247–266.

Curran, P.J., Dungan, J.L., Macler, B.A. & Plummer, S.E. 1991. The effect of a red leaf pigment on the relationship between red edge and chlorophyll concentration. *Remote Sensing of Environment* 35: 69–76.

Damm, A., Kneubühler, M., Schaepman, M.E. & Rascher, U. 2012. Evaluation of gross primary production (GPP)

variability over several ecosystems in Switzerland using sun-induced chlorophyll fluorescence derived from APEX data. In: *Proceedings of Geoscience and Remote Sensing Symposium (IGARSS)*, pp. 7133–7136. 2012 IEEE International, doi: 10.1109/IGARSS.2012.6352018, Available at: http://ieeexplore.ieee.org/stamp/stamp.jsp?tp=&arnumber=6352018&isnumber=6350328

De Jager, N.R. & Pastor, J. 2009. Declines in moose population density at Isle Royle National Park, MI, USA and accompanied changes in landscape patterns. *Landscape Ecology* 24: 1389–1403.

De Knegt, H.J., Groen, T.A., Van De Vijver, C.A.D.M., Prins, H.H.T. & Van Langevelde, F. 2008. Herbivores as architects of savannas: inducing and modifying spatial vegetation patterning. *Oikos* 117: 543–554.

Epstein, H.E., Burke, I.C. & Lauenroth, W.K. 2002. Regional patterns of decomposition and primary production rates in the U.S. Great Plains. *Ecology* 83: 320–327.

Fava, F., Colombo, R., Bocchi, S., Meroni, M., Sitzia, M., Fois, N. & Zucca, C. 2009. Identification of hyperspectral vegetation indices for Mediterranean pasture characterization. *International Journal of Applied Earth Observation and Geoinformation* 11: 233–243.

Frank, D.A., Inouye, R.S., Huntly, N., Minshall, G.W. & Anderson, J.E. 1994. The biogeochemistry of a north-temperate grassland with native ungulates: nitrogen dynamics in Yellowstone National Park. *Biogeochemistry* 26: 163–188.

Frank, D.A., Depriest, T., McLauchlan, K. & Risch, A.C. 2011. Topographic and ungulate regulation of soil C turnover in a temperate grassland ecosystem. *Global Change Biology* 17: 495–504.

Gamon, J.A., Field, C.B., Roberts, D.A., Ustin, S.L. & Valentini, R. 1993. Functional patterns in an annual grassland during an AVIRIS overflight. *Remote Sensing of Environment* 44: 239–253.

Gobron, N. 1997. Theoretical limits to the estimation of the leaf area index on the basis of visible and near-infrared remote sensing data. *IEEE Transactions on Geoscience and Remote Sensing* 35: 1438–1445.

Goetz, A.F.H. 2009. Three decades of hyperspectral remote sensing of the Earth: a personal view. *Remote Sensing of Environment* 113: S5–S16.

Goetz, A.F.H., Vane, G., Solomon, J.E. & Rock, B.N. 1985. Imaging spectrometry for earth remote sensing. *Science* 228: 1147–1153.

Haboudane, D., Miller, J.R., Pattey, E., Zarco-Tejada, P.J. & Strachan, I.B. 2004. Hyperspectral vegetation indices and novel algorithms for predicting green LAI of crop canopies: modeling and validation in the context of precision agriculture. *Remote Sensing of Environment* 90: 337–352.

Hansen, P.M. & Schjoerring, J.K. 2003. Reflectance measurement of canopy biomass and nitrogen status in wheat crops using normalized difference vegetation indices and partial least squares regression. *Remote Sensing of Environment* 86: 542–553.

He, Y., Guo, X. & Wilmshurst, J. 2006. Studying mixed grassland ecosystems I: suitable hyperspectral vegetation indices. *Canadian Journal of Remote Sensing* 32: 98–107.

He, K.S., Rocchini, D., Neteler, M. & Nagendra, H. 2011. Benefits of hyperspectral remote sensing for tracking plant invasions. *Diversity and Distributions* 17: 381–392.

Hebblewhite, M. & Haydon, D.T. 2010. Distinguishing technology from biology: a critical review of the use of GPS telemetry data in ecology. *Philosophical Transactions of the Royal Society B: Biological Sciences* 365: 2303–2312.

Hill, M.J. 2004. Grazing agriculture: managed pasture, grassland, and rangeland. In: Ustin, S.L. (ed.) *Manual of remote sensing: remote sensing for natural resource management and environmental monitoring*, pp. 449–530. Wiley, Hoboken, NJ, US.

Horler, D.N.H., Dockray, M. & Barber, J. 1983. The red edge of plant leaf reflectance. *International Journal of Remote Sensing* 4: 273–288.

Huete, A. & Jackson, R. 1988. Soil and atmosphere influences on the spectra of partial canopies. *Remote Sensing of Environment* 25: 89–105.

Jehle, M., Hueni, A., Damm, A., D'Odorico, P., Weyermann, J., Kneubühler, M., Schläpfer, D., Schaepman, M.E. & Meuleman, K. 2010. APEX – Current status, performance and validation concept. In: *Proceedings of Sensors, 2010 IEEE*, pp. 533–537. doi: 10.1109/ICSENS.2010.5690122, Available at: http://ieeexplore.ieee.org/stamp/stamp.jsp?tp=&arnumber=5690122&isnumber=5689839

Jiang, C., Zhao, H. & Jia, G. 2012. Estimation of adjacency effect in the remotely sensed Hyperspectral data over rugged scenes. In: *Proceedings of: 2012 IEEE International Conference on Imaging Systems and Techniques (IST)*, pp. 195–199, doi: 10.1109/IST.2012.6295550, Available at: http://ieeexplore.ieee.org/stamp/stamp.jsp?tp=&arnumber=6295550&isnumber=6295479

Jones, H.G. & Vaughan, R.A. 2010. *Remote sensing of vegetation: principles, techniques, and applications*. Oxford University Press, New York, NY, US.

Kerr, J.T. & Ostrovsky, M. 2003. From space to species: ecological applications for remote sensing. *Trends in Ecology & Evolution* 18: 299–305.

Knapp, A.K., Fahnestock, J.T., Hamburg, S.P., Statland, L.B., Seastedt, T.R. & Schimel, D.S. 1993. Landscape patterns in soil–plant water relations and primary production in tallgrass prairie. *Ecology* 74: 549–560.

Knapp, A.K., Fay, P.A., Blair, J.M., Collins, S.L., Smith, M.D., Carlisle, J.D., Harper, C.W., Danner, B.T., Lett, M.S. & McCarron, J.K. 2002. Rainfall variability, carbon cycling, and plant species diversity in a mesic grassland. *Science* 298: 2202–2205.

Lauenroth, W.K. & Sala, O.E. 1992. Long-term forage production of North American shortgrass steppe. *Ecological Applications* 2: 397–403.

Liu, J., Pattey, E., Miller, J.R., McNairn, H., Smith, A. & Hu, B. 2010. Estimating crop stresses, aboveground dry biomass

and yield of corn using multi-temporal optical data combined with a radiation use efficiency model. *Remote Sensing of Environment* 114: 1167–1177.

Lu, D. 2006. The potential and challenge of remote sensing-based biomass estimation. *International Journal of Remote Sensing* 27: 1297–1328.

McNaughton, S.J. 1979. Grazing as an optimization process: grass-ungulate relationships in the serengeti. *The American Naturalist* 113: 691–703.

McNaughton, S.J., Banyikwa, F.F. & McNaughton, M.M. 1997. Promotion of the cycling of diet-enhancing nutrients by African grazers. *Science* 278: 1798–1800.

MeteoSwiss 2013. *IDAweb. The data portal of MeteoSwiss for research and teaching*. http://www.meteoschweiz.admin.ch/web/de/services/datenportal/idaweb.html. Accessed 12 March 2013.

Middleton, E.M. 1991. Solar zenith angle effects on vegetation indices in tallgrass prairie. *Remote Sensing of Environment* 38: 45–62.

Milton, E.J., Schaepman, M.E., Anderson, K., Kneubühler, M. & Fox, N. 2009. Progress in field spectroscopy. *Remote Sensing of Environment* 113: S92–S109.

Mirik, M., Norland, J.E., Crabtree, R.L. & Biondini, M.E. 2005. Hyperspectral one-meter-resolution remote sensing in Yellowstone National Park, Wyoming: II. Biomass. *Rangeland Ecology and Management* 58: 459–465.

Myneni, R.B., Hall, F.G., Sellers, P.J. & Marshak, A.L. 1995. Interpretation of spectral vegetation indexes. *IEEE Transactions on Geoscience and Remote Sensing* 33: 481–486.

Numata, I., Roberts, D.A., Chadwick, O.A., Schimel, J., Sampaio, F.R., Leonidas, F.C. & Soares, J.V. 2007. Characterization of pasture biophysical properties and the impact of grazing intensity using remotely sensed data. *Remote Sensing of Environment* 109: 314–327.

Numata, I., Roberts, D.A., Chadwick, O.A., Schimel, J.P., Galvão, L.S. & Soares, J.V. 2008. Evaluation of hyperspectral data for pasture estimate in the Brazilian Amazon using field and imaging spectrometers. *Remote Sensing of Environment* 112: 1569–1583.

Oldeland, J., Dorigo, W., Lieckfeld, L., Lucieer, A. & Jürgens, N. 2010. Combining vegetation indices, constrained ordination and fuzzy classification for mapping semi-natural vegetation units from hyperspectral imagery. *Remote Sensing of Environment* 114: 1155–1166.

Richter, R. & Schläpfer, D. 2002. Geo-atmospheric processing of airborne imaging spectrometry data. Part 2: atmospheric/topographic correction. *International Journal of Remote Sensing* 23: 2631–2649.

Risch, A.C. & Frank, D.A. 2006. Carbon dioxide fluxes in a spatially and temporally heterogeneous temperate grassland. *Oecologia* 147: 291–302.

Risch, A.C., Schütz, M., Krüsi, B.O., Kienast, F., Wildi, O. & Bugmann, H. 2004. Detecting successional changes in long-term empirical data from subalpine conifer forests. *Plant Ecology* 172: 95–105.

Risch, A.C., Jurgensen, M.F. & Frank, D.A. 2007. Effects of grazing and soil micro-climate on decomposition rates in a spatio-temporally heterogeneous grassland. *Plant and Soil* 298: 191–201.

Risch, A.C., Jurgensen, M.F., Page-Dumroese, D.S., Wildi, O. & Schütz, M. 2008. Long-term development of above- and below-ground carbon stocks following land-use change in subalpine ecosystems of the Swiss National Park. *Canadian Journal of Forest Research* 38: 1590–1602.

Risch, A.C., Haynes, A.G., Busse, M.D., Filli, F. & Schütz, M. 2013. The response of soil CO_2 fluxes to progressively excluding vertebrate and invertebrate herbivores depends on ecosystem type. *Ecosystems* 16: 1192–1202.

Ritchie, M.E. & Olff, H. 1999. Spatial scaling laws yield a synthetic theory of biodiversity. *Nature* 400: 557–560.

Roberts, D.A., Smith, M.O. & Adams, J.B. 1993. Green vegetation, nonphotosynthetic vegetation, and soils in AVIRIS data. *Remote Sensing of Environment* 44: 255–269.

Rouse, J.W. Jr, Haas, R.H., Deering, D.W., Schell, J.A. & Harlan, J.C. 1974. *Monitoring the vernal advancement and retrogradation (Green Wave Effect) of natural vegetation*. NASA/GSFC Final report, Greenbelt, MD, USA.

Schaepman, M.E., Ustin, S.L., Plaza, A.J., Painter, T.H., Verrelst, J. & Liang, S. 2009. Earth system science related imaging spectroscopy – An assessment. *Remote Sensing of Environment* 113: S123–S137.

Schaepman-Strub, G., Schaepman, M.E., Painter, T.H., Dangel, S. & Martonchik, J.V. 2006. Reflectance quantities in optical remote sensing – definitions and case studies. *Remote Sensing of Environment* 103: 27–42.

Schläpfer, D. & Richter, R. 2002. Geo-atmospheric processing of airborne imaging spectrometry data. Part 1: parametric orthorectification. *International Journal of Remote Sensing* 23: 2609–2630.

Schmidtlein, S., Feilhauer, H. & Bruelheide, H. 2012. Mapping plant strategy types using remote sensing. *Journal of Vegetation Science* 23: 395–405.

Schütz, M., Risch, A.C., Leuzinger, E., Krüsi, B.O. & Achermann, G. 2003. Impact of herbivory by red deer (*Cervus elaphus* L.) on patterns and processes in subalpine grasslands in the Swiss National Park. *Forest Ecology and Management* 181: 177–188.

Schütz, M., Risch, A.C., Achermann, G., Thiel-Egenter, C., Page-Dumroese, D.S., Jurgensen, M.F. & Edwards, P.J. 2006. Phosphorus translocation by red deer on a subalpine grassland in the central European Alps. *Ecosystems* 9: 624–633.

Senft, R.L., Coughenour, M.B., Bailey, D.W., Rittenhouse, L.R., Sala, O.E. & Swift, D.M. 1987. Large herbivore foraging and ecological hierarchies. *BioScience* 37: 789–799.

Sims, D.A. & Gamon, J.A. 2002. Relationships between leaf pigment content and spectral reflectance across a wide range of species, leaf structures and developmental stages. *Remote Sensing of Environment* 81: 337–354.

Skidmore, A.K. & Ferwerda, J.G. 2008. Resource distribution and dynamics: mapping herbivore resources. In: Prins, H.H.T. & Van Langevelde, F. (eds.) *Resource ecology: spatial and temporal dynamics of foraging*, pp. 57–77. Springer, Dordrecht, NL.

Skidmore, A.K., Ferwerda, J.G., Mutanga, O., Van Wieren, S.E., Peel, M., Grant, R.C., Prins, H.H.T., Balcik, F.B. & Venus, V. 2010. Forage quality of savannas – Simultaneously mapping foliar protein and polyphenols for trees and grass using hyperspectral imagery. *Remote Sensing of Environment* 114: 64–72.

Spalinger, L.C., Haynes, A.G., Schütz, M. & Risch, A.C. 2012. Impact of wild ungulate grazing on Orthoptera abundance and diversity in subalpine grasslands. *Insect Conservation and Diversity* 5: 444–452.

Suter, W., Suter, U., Krüsi, B. & Schütz, M. 2004. Spatial variation of summer diet of red deer *Cervus elaphus* in the eastern Swiss Alps. *Wildlife Biology* 10: 43–50.

Tanentzap, A.J. & Coomes, D.A. 2012. Carbon storage in terrestrial ecosystems: do browsing and grazing herbivores matter? *Biological Reviews* 87: 72–94.

Thenkabail, P.S., Smith, R.B. & De Pauw, E. 2000. Hyperspectral vegetation indices and their relationships with agricultural crop characteristics. *Remote Sensing of Environment* 71: 158–182.

Thenkabail, P.S., Smith, R.B. & De Pauw, E. 2002. Evaluation of narrowband and broadband vegetation indices for determining optimal hyperspectral wavebands for agricultural crop characterization. *Photogrammetric Engineering and Remote Sensing* 68: 607–621.

Thiel-Egenter, C., Risch, A.C., Jurgensen, M.F., Page-Dumroese, D.S., Krüsi, B.O. & Schütz, M. 2007. Response of a subalpine grassland to simulated grazing: aboveground productivity along soil phosphorus gradients. *Community Ecology* 8: 111–117.

Todd, S.W., Hoffer, R.M. & Milchunas, D.G. 1998. Biomass estimation on grazed and ungrazed rangelands using spectral indices. *International Journal of Remote Sensing* 19: 427–438.

Tucker, C.J. 1977. Asymptotic nature of grass canopy spectral reflectance. *Applied Optics* 16: 1151–1156.

Tucker, C.J. 1979. Red and photographic infrared linear combinations for monitoring vegetation. *Remote Sensing of Environment* 8: 127–150.

Turner, C.L., Blair, J.M., Schartz, R.J. & Neel, J.C. 1997. Soil N and plant responses to fire, topography, and supplemental N in tallgrass prairie. *Ecology* 78: 1832–1843.

Ustin, S.L. & Gamon, J.A. 2010. Remote sensing of plant functional types. *New Phytologist* 186: 795–816.

Ustin, S.L., Roberts, D.A., Gamon, J.A., Asner, G.P. & Green, R.O. 2004. Using imaging spectroscopy to study ecosystem processes and properties. *BioScience* 54: 523–534.

Verrelst, J., Schaepman, M.E., Malenovský, Z. & Clevers, J.G.P.W. 2010. Effects of woody elements on simulated canopy reflectance: implications for forest chlorophyll content retrieval. *Remote Sensing of Environment* 114: 647–656.

Wang, K., Franklin, S.E., Guo, X. & Cattet, M. 2010. Remote sensing of ecology, biodiversity and conservation: a review from the perspective of remote sensing specialists. *Sensors* 10: 9647–9667.

Wardle, D.A., Bardgett, R.D., Klironomos, J.N., Setälä, H., Van Der Putten, W.H. & Wall, D.H. 2004. Ecological linkages between aboveground and belowground biota. *Science* 304: 1629–1633.

Westoby, M., Falster, D.S., Moles, A.T., Vesk, P.A. & Wright, I.J. 2002. Plant ecological strategies: some leading dimensions of variation between species. *Annual Review of Ecology and Systematics* 33: 125–159.

Wright, I.J., Reich, P.B. & Westoby, M. 2001. Strategy shifts in leaf physiology, structure and nutrient content between species of high- and low-rainfall and high- and low-nutrient habitats. *Functional Ecology* 15: 423–434.

Youngentob, K.N., Renzullo, L.J., Held, A.A., Jia, X., Lindenmayer, D.B. & Foley, W.J. 2012. Using imaging spectroscopy to estimate integrated measures of foliage nutritional quality. *Methods in Ecology and Evolution* 3: 416–426.

Zarco-Tejada, P.J., Ustin, S.L. & Whiting, M.L. 2005. Temporal and spatial relationships between within-field yield variability in cotton and high-spatial hyperspectral remote sensing imagery. *Agronomy Journal* 97: 641–653.

Zheng, S., Ren, H., Li, W. & Lan, Z. 2012. Scale-dependent effects of grazing on plant C: N: P stoichiometry and linkages to ecosystem functioning in the inner Mongolia Grassland. *PLoS One* 7: e51750.

Doi: 10.1111/jvs.12214